Supplementary Information section for:

A simple method for evaluating photochemical dependencies in the atmosphere

Katja Džepina[1,2,3] and Sasha Madronich[1]*

[1]National Center for Atmospheric Research, Atmospheric Chemistry Division, 1850 Table Mesa Drive, PO Box 3000, Boulder, CO 80305, USA

[2]Rudjer Bošković Institute, Physical Chemistry Division, Laboratory for Chemical Kinetics and Atmospheric Chemistry, Bijenička cesta 54, PO Box 180, HR-10002 Zagreb, Croatia

[3]PSI Center for Energy and Environmental Sciences, 5232 Villigen PSI, Switzerland

Supplementary Information section summary:

Total number of SI pages: 10

Number of pages of SI text: 5

Number of SI figures: 3

***Corresponding author**: Sasha Madronich <sasha@ucar.edu>

S1 Box model simulations of photo-chemical budgets for OH, RO_x and O_x

Computed diurnal evolutions of key species are shown in Figure 1 of the main text. Box model simulations of gas-phase chemical species in the conditions of remote atmosphere were performed in order to gain an understanding of behavior of species studied in this work. The model-calculated budgets for HO, RO_x (OH + HO_2 + RO_2) and O_x (O_3 + NO_2) are shown in Figure 1. The budgets are shown for the fifth day of the simulation so as to give other non-fixed intermediates enough time to reach near steady state conditions. The loss of OH averaged over the fifth diurnal cycle is dominated by CO (75%) with a minor contribution from CH_4 (13%). Less than 5% of the OH loss is due to NMHCs and oxygenated organic intermediates in this pristine environment. In most cases, these OH losses produce peroxy radicals, HO_2 and RO_2. The OH production terms include HO_2+NO (35%), HO_2+O_3 (34%), and O^1D+H_2O (26%), with only a minor contribution from hydrogen peroxide (H_2O_2) photolysis (3.7%). The loss of RO_x averaged over the fifth diurnal cycle is dominated by HO_2 self-reaction (64%) with a minor contribution from CH_3O_2+HO_2 (26%). The production of RO_x is dominated by O^1D+H_2O (57%) with contributions from HCHO photolysis (20%) and H_2O_2 photolysis (8.1%). The production of O_x over the fifth diurnal cycle is dominated by HO_2+NO (73%) and RO_2+NO (24%). Loss of O_x is dominated by HO_2+O_3 (63%) with contributions from O^1D+H_2O (24%) and OH+O_3 (12%). The net rate of change over the fifth simulation day is small, with near balance between production and loss (-0.12 ppbv/day).

Direct evaluation of the modeled HO_x, RO_x, and O_x budgets with observations is difficult because production and loss rates are not measured directly. We note that the small net production of O_x is consistent with the observation that O_3 concentrations were relatively steady during TOPSE. However, we also note that the calculated budget of HO_2 radicals is problematic *vis-à-vis* H_2O_2 measurements (see Table 2), which are well below 1 ppb with average ~ 320 ppt and medians considerably lower, near 100 ppt. The model (see Fig. 1b)

suggests stronger H_2O_2 production, approx. 2.5 ppb/day at noon or, taken over a diurnal cycle, about 1 ppb per day. With this large production, the low measured concentrations point to an H_2O_2 lifetime of approx. 1/3rd of a day, much shorter than the diurnally averaged lifetimes estimated for H_2O_2 loss by photolysis (approx. 2 days) and by OH (approx. 13 days). This may be pointing to the importance of heterogeneous losses of H_2O_2 being dominant under these selected TOPSE conditions. The fact that measured CH_3OOH levels are comparable to H_2O_2 levels, while the gas-phase model predicts much smaller CH_3OOH/H_2O_2 ratios, is consistent with this explanation, given the higher solubility of H_2O_2. An alternative interpretation is that the box model overestimates HO_2 radical concentrations, the predicted H_2O_2 production of course being proportional to $[HO_2]^2$.

S2 Box model calculations of sensitivity coefficients used for LSFs

The model-calculated sensitivity coefficients are given in Table 3, can be negative, and have small ranges (shown as errors in Table 3) over the large variations explored. The detailed sensitivities can be understood easily, at least qualitatively, in terms of the known photochemistry occurring in the pristine troposphere, as detailed below.

J values: Photolysis reactions are the sources of most HO_x radicals. Based on Fig. 1c, the most important of these are:

$$H_2O_2 + h\nu \rightarrow OH + OH \quad \text{(RS1)}$$

$$O_3 + h\nu \rightarrow O_2 + O(^1D)\ (+H_2O) \rightarrow O_2 + 2\ OH \quad \text{(RS2)}$$

$$CH_3OOH + h\nu \rightarrow OH + CH_3O\ (+ O_2) \rightarrow OH + HO_2 + CH_2O \quad \text{(RS3)}$$

$$CH_2O + h\nu \rightarrow H + HCO\ (+ 2\ O_2) \rightarrow 2\ HO_2 + CO \quad \text{(RS4)}$$

Two HO_x radicals are produced in each case. This production is balanced (see Fig. 1c) by peroxy radical reactions (RS5-6) and to a lesser extent the OH termination reaction (RS5):

$$HO_2 + HO_2 \rightarrow H_2O_2 + O_2 \quad \text{(RS5)}$$

$HO_2 + CH_3O_2 \rightarrow CH_3OOH$ (RS6)

$OH + NO_2 \rightarrow HNO_3$ (RS7)

Neglecting the organic terms, the HO_x rate equation is

$$\frac{d[HO_x]}{dt} = 2J_1[H_2O_2] + 2J_2[O_3]f[H_2O] - 2k_5[HO_2]^2 - k_7[OH][NO_2] \quad \text{(Eq. S1)}$$

where *f* is related to the probability of $O(^1D)$ reacting with water rather than being quenched. In low NO_x conditions, the last term is relatively small, so at steady state:

$$[HO_2] = \sqrt{\frac{J_1[H_2O_2]+J_2[O_3]f[H_2O]}{k_5}} \quad \text{(Eq. S2)}$$

This square root dependence is well borne-out for peroxy radicals in Table 3. However, the stronger, nearly linear increase in OH is due to the increase in another photolysis reaction,

$NO_2 + h\nu \rightarrow NO + O(^3P)\ (+O_2) \rightarrow NO + O_3$ (RS8)

Table 3 shows that increasing *J* values result in an almost linear increase in the NO/NO_2 ratio, with the higher NO levels (at constant NO_x) then leading to OH reformation via the reaction:

$NO + HO_2 \rightarrow NO_2 + OH$ (RS9)

Water (H_2O): Increased water concentrations lead to a larger fraction of $O(^1D)$ reacting to form OH:

$H_2O + O(^1D) \rightarrow 2OH$ (RS10)

This reaction is a significant but not unique source of HO_x radicals, with photolysis of peroxides being at times comparable or even more important. Thus, the effect on HO_2 and RO_2 (the major HO_x constituents) falls below the square root dependence found, e.g., for *J* values, as is also clear from Eq. S2. The small negative effect on the NO/NO_2 ratio results from the reaction of NO with increased peroxy radical amounts.

Nitrogen oxides (NO_x): Increases in NO_x are seen to have little effect on the NO/NO_2 partitioning, or, conversely, model-predicted NO/NO_2 ratios are insensitive to the exact NO_x level. The availability of more NO_x does lead to more OH production, e.g., if added as NO:

$$NO + HO_2 \rightarrow OH + NO_2 \quad \text{(RS11)}$$

but this is also a loss for HO_2, which is closely coupled to OH by the CO reaction:

$$OH + CO\ (+ O_2) \rightarrow HO_2 + CO_2 \quad \text{(RS12)}$$

To the extent that these two reactions contribute to HO_x partitioning, the HO_2/OH ratio should scale as CO/NO. Thus, higher NO_x levels lead to higher OH, to constant HO_2 values, and to negative RO_2 changes. This last effect results from the reaction:

$$NO + RO_2 \rightarrow \text{products} \quad \text{(RS13)}$$

being more important for RO_2 than for HO_2, due to the absence of the organic analogue to the reaction:

$$HO_2 + O_3 \rightarrow OH + 2\ O_2 \quad \text{(RS14)}$$

Adding NO_x as NO_2, provides some additional reactivity through ozone formation.

Ozone (O_3): Ozone affects radical production via direct photolysis (as already discussed for H_2O and J sensitivities), and affects the NO_x photostationary state:

$$\frac{[NO]}{[NO_2]} = \frac{J_5}{k_4[HO_2]+k_5[RO_2]+k_6[O_3]} \quad \text{(Eq. S3)}$$

Of the three terms in denominator, HO_2 and RO_2 are negligible compared to O_3 for these conditions (see model simulations in Fig. 1). Thus the NO/NO_2 ratio is nearly proportional to J_5/O_3.

Carbon monoxide (CO): Increases in CO are seen to decrease OH substantially, in accord with Fig. 1 that shows their direct reaction to be a major part of the total OH budget. The decrease in OH results in lower oxidation rates for hydrocarbons, and thus fewer RO_2's produced. The increase in the number of HO_2 is equal to the number (not the percent) decrease of RO_2 produced, at least within the rough approximations that OH losses are always accompanied by production of either HO_2 or RO_2, and these having similar lifetimes. Therefore, the total, HO_2+RO_2, remains constant, as does the NO/NO_2 ratio. Little if any additional ozone production or destruction would be expected by addition of CO.

Temperature (T): The rate constants for the important reactions OH + CH_4 and for NO + O_3 both increase strongly with temperature, resulting in faster RO_2 production and smaller NO/NO_2 ratios.

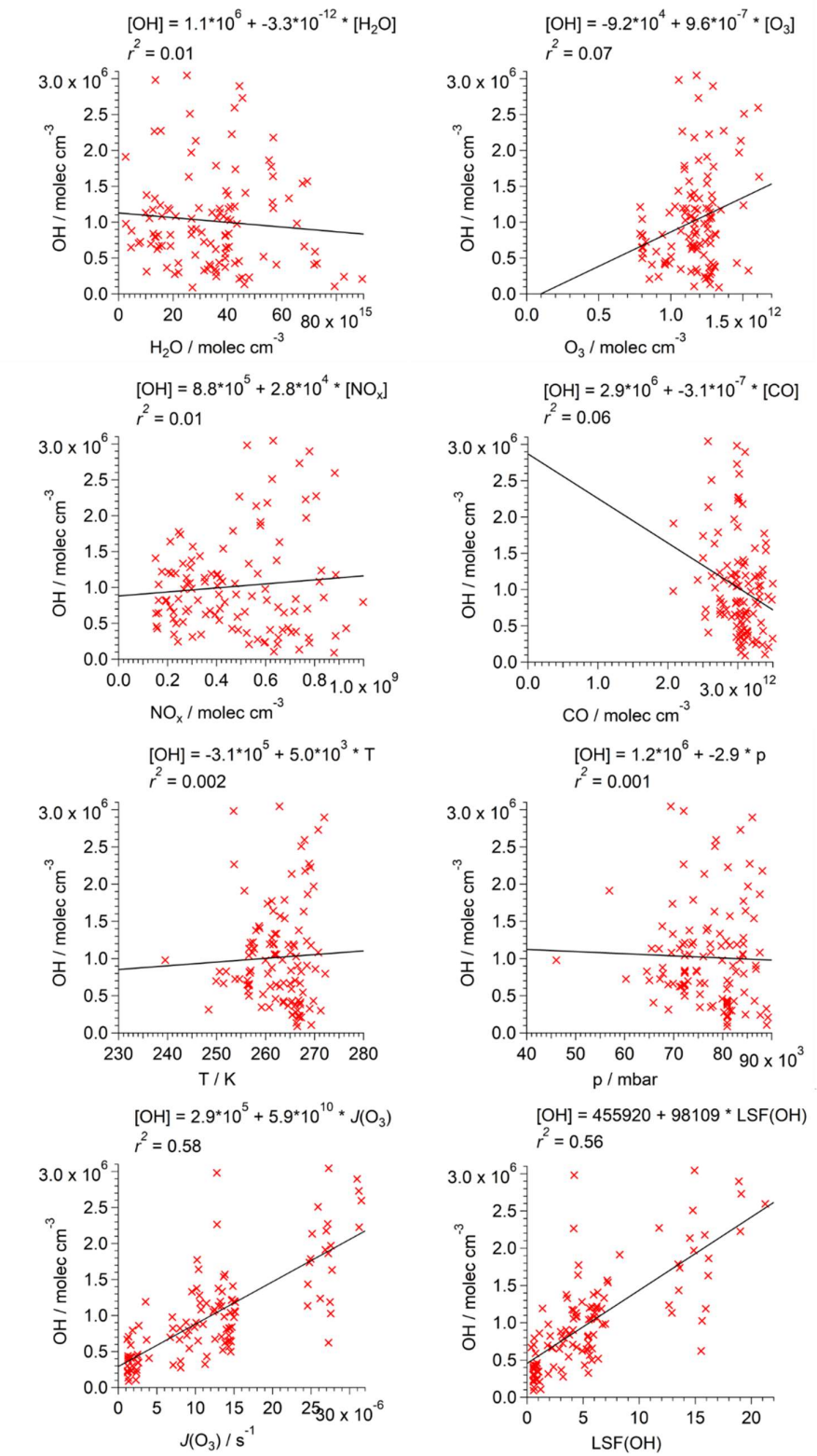

Figure S1. Correlations of OH with TOPSE-measured species (H_2O, O_3, NO_x and CO) and meteorological parameters (T and p) used in LSF. Also given are correlations of OH with *J* value ($O_3 + h\nu \rightarrow O_2 + O(^1D)$) and LSF (bottom two panels) shown in Figure 3 of the main text, for the ease of direct comparisons.

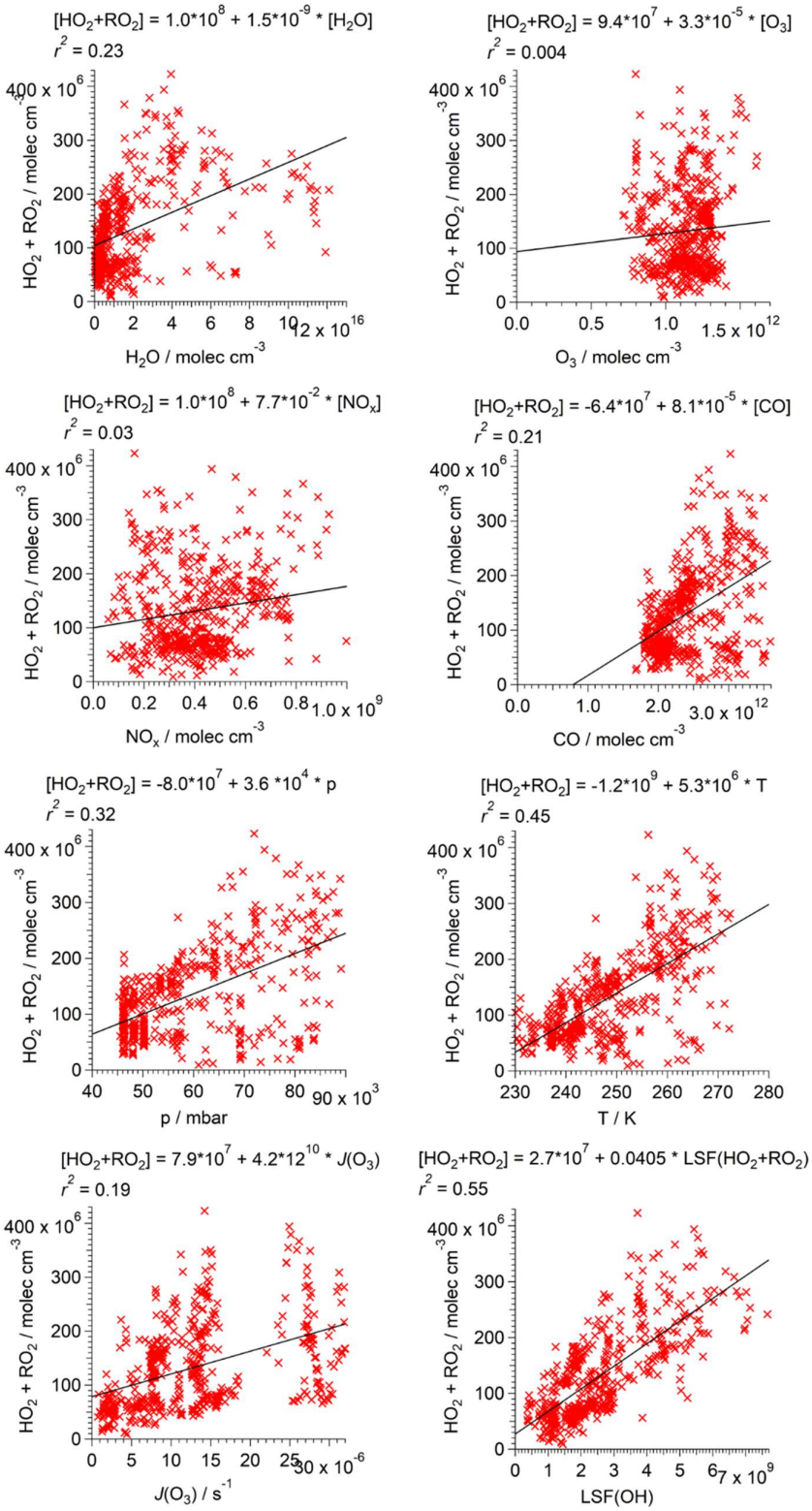

Figure S2. Correlations of $HO_2 + RO_2$ with TOPSE-measured species (H_2O, O_3, NO_x and CO) and meteorological parameters (T and p) used in LSF. Also given are correlations of $HO_2 + RO_2$ with J value ($O_3 + h\nu \rightarrow O_2 + O(^1D)$) and LSF (bottom two panels) shown in Figure 3 of the main text, for the ease of direct comparisons.

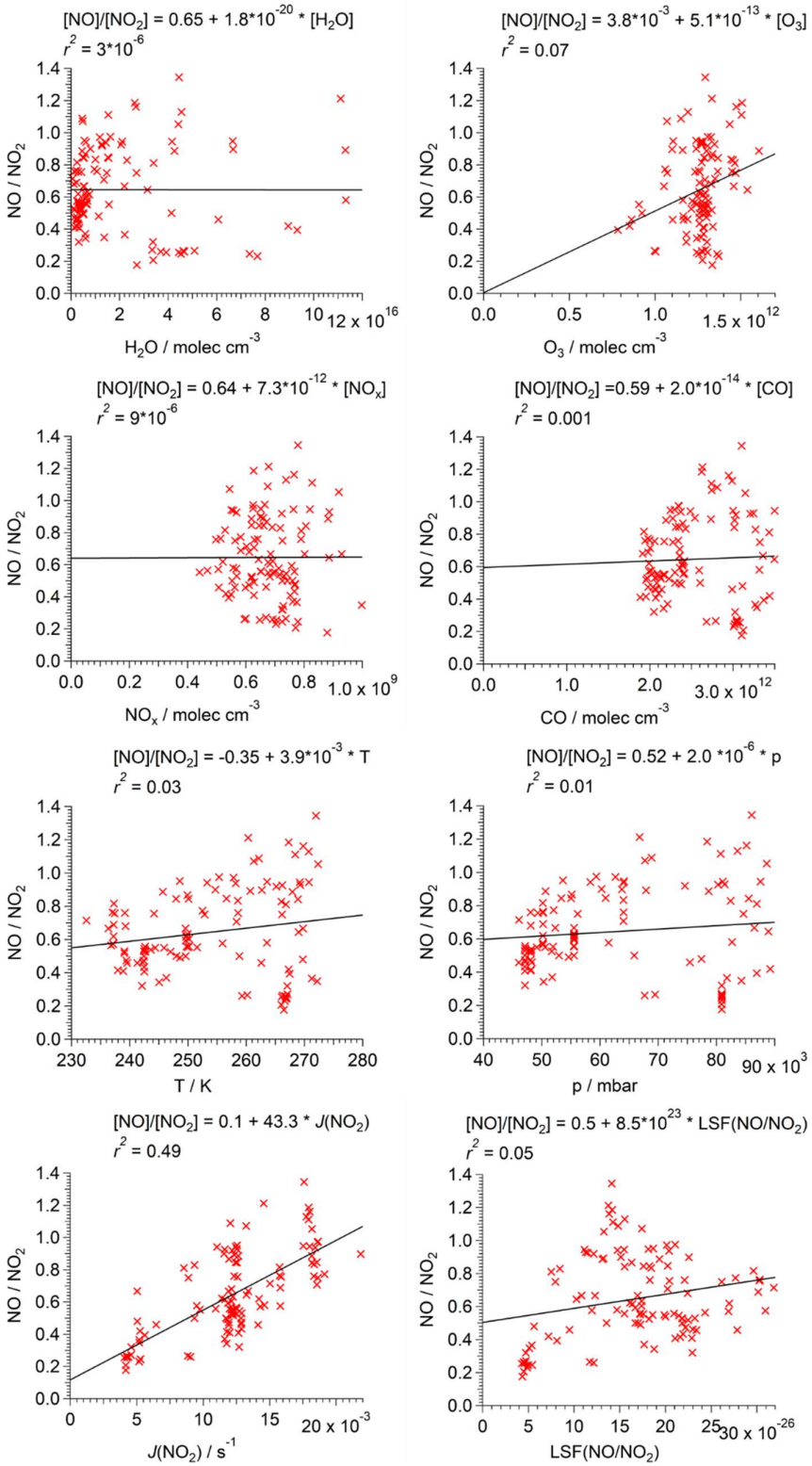

Figure S3. Correlations of NO/NO_2 ratio with TOPSE-measured species (H_2O, O_3, NO_x and CO) and meteorological parameters (T and p) used in LSF. Also given are correlations of NO/NO_2 with J value ($NO_2 + h\nu \rightarrow NO + O(^3P)$) and LSF (bottom two panels) shown in Figure 3 of the main text, for the ease of direct comparisons.